Facility-Dependent Effects in Shock Tubes

Damien Nativel, Mustapha Fikri, Christof Schulz
IVG, Institute for Combustion and Gas Dynamics – Reactive Fluids,
University of Duisburg-Essen, 47048 Duisburg, Germany

Sean P. Cooper, Eric L. Petersen
Texas A&M University
College Station, Texas, USA

1 Introduction

In an ideal shock-tube experiment, the incident shock wave propagates through the driven section at a constant velocity. However, in real shock tubes, the incident-shock velocity is transient, decreasing with axial position in the propagation direction. This attenuation of the incident shock wave (ISW) is generally linear near the endwall of the driven section and is caused by boundary-layer growth behind the ISW [1-3]. Attenuation is generally calculated as the percent change in velocity per unit length (%/m). A linear fit can be made of the ISW velocity, and the resulting velocity at the endwall can be extrapolated. This velocity can then be used for calculating conditions behind the reflected shock wave in region 5 (T_5, p_5, etc.). These conditions, according to ideal shock-wave theory, should stay constant until the arrival of the expansion wave. In real shock tubes, region 5 is compressed further again due to boundary-layer growth [4-6]. This generally linear increase in p_5 with time is defined as the change in pressure with time normalized by the test-gas pressure (p_5). It is given in units of percent per millisecond (%/ms) and is referred to hereafter as dp*/dt. These dp*/dt effects can be mitigated using a variety of previously established methods that are described in detail elsewhere [7-9]. Conversely, these effects can be exacerbated by shock-tube facility design and, for pressure-driven shock tubes, non-ideal diaphragm bursting.

Pressure-driven shock tubes utilize a diaphragm, which separates the driver and driven sections, to compress the driven gas. To initiate a shock-tube experiment, the driver section is continually filled until the diaphragm ruptures (at a pressure specific to that diaphragm's material and thickness). At rupture, a contact surface between the high-pressure (driver) and low-pressure (driven) gases is created, which acts as a piston compressing the driven gas and initiating shock propagation. Ideal behavior of a shock-tube facility heavily depends on the facility's ability to burst diaphragms quickly and uniformly. In the theoretical case, the diaphragm is instantaneously removed, creating a uniform contact surface. However, in a real experiment the diaphragm takes time to burst and occupies space during rupture. These real behaviors can cause significant deviation from theory [10-12].

Correspondence to: damien.nativel@uni-due.de

The present paper describes a series of experiments using multiple facilities within two laboratories; the goal of these tests was to generate and study a large data set pertaining to incident-shock attenuation and non-ideal diaphragm bursting effects. We first provide an overview of the facilities and data acquisition, followed by a presentation of the experimental results. A brief discussion is then provided.

2 Shock-Tube Facilities and Data Acquisition

A recent study was performed at two shock-tube laboratories, namely the Institute for Combustion and Gas Dynamics – Reactive Fluids at the University of Duisburg-Essen (UDE) and Texas A&M University (TAMU) to characterize the dependence of non-ideal effects on shock-tube facilities. The study involved four shock tubes, two at each laboratory. The facilities utilized at UDE included a conventional shock tube (CST) and a high-pressure shock tube (HPST). Both shock tubes have a constant inner diameter (ID). Facilities utilized at TAMU included the Aerospace shock tube (AST) and the high-pressure shock tube (HPST). Both TAMU shock tubes have a diverging nozzle downstream of the diaphragm section, as the ID of the driven section is greater than that of the driver section. The dimensions of the driven sections for these shock-tube facilities are shown in Table 1. More detailed descriptions of these facilities can be found elsewhere [13-16].

Table 1: Dimensions of shock-tube facilities.

		Driven	
		ID (cm)	Length (m)
TAMU	AST	16.20	7.88
	HPST	15.24	5.03
UDE	CST	8.00	8.00
	HPST	9.00	6.10

For this study, attenuation data were taken using five pressure transducers for the TAMU and four for the UDE experiments to gather four and three velocity intervals, respectively. A least-squares method was used to obtain a linear fit of the velocity data. The slope of this curve was then used to calculate ISW attenuation. Attenuation data were gathered from all four facilities across a range of pressures and incident-shock Mach numbers in argon and nitrogen. As part of this study, the effect of diaphragm bursting time on non-ideal effects (ISW attenuation and dp^*/dt) and its facility dependence were investigated. The bursting time is the time span from the initial pressure rise in the driver section until the rupture of the diaphragm. During this time, the driver section is pressurized with a constant flow of driver gas. To this end, measurements of incident-shock attenuation and dp^*/dt were taken with varying driver filling rates. Helium was used as driver gas for all experiments.

ISW attenuation data were taken for test-gas pressures (p_5) between 1 and 25 bar for Mach numbers between 2.1 and 3.1 for Ar, and between 2.1 and 4.1 for N_2. The data are shown in Fig. 1. These plots show no significant dependence of ISW attenuation on Mach number, even though it is the most significant parameter for boundary-layer growth. Wide scatter is seen for all facilities, although a clear difference between laboratories can be seen. On average, ISW attenuation values of about 2.1 %/m and 0.8 %/m were seen for UDE and TAMU, respectively. The higher attenuation values seen at UDE are indicative of the smaller ID relative to the TAMU shock tubes, because for the same shock conditions, the boundary layer occupies a larger percentage of the tube's cross section in the smaller UDE tubes. It should be noted that the experiments at higher Mach number $M_1 > 3$ (see Fig. 1b) for N_2 at TAMU should not be considered for comparison due to the lack of similar experiments at UDE.

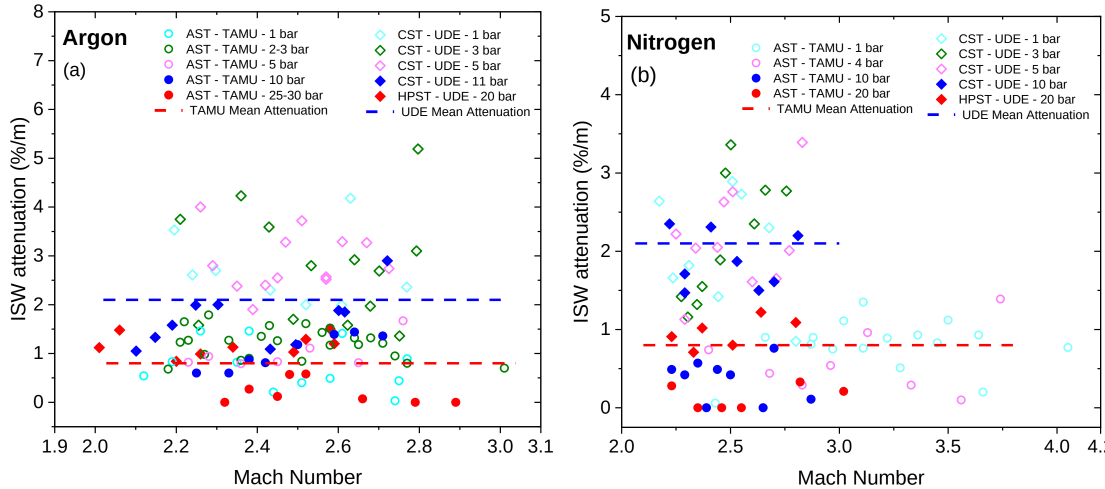

Figure 1. (a) ISW attenuation data for Ar, (b) ISW attenuation data for N_2. Diamonds and circles represent UDE and TAMU data, respectively. p_5 values are color coded to link the data for all facilities. Average ISW attenuation values are shown as dashed lines.

ISW attenuation and dp*/dt values collected for the diaphragm bursting time investigation are shown in Fig. 2. It should be noted that diaphragm bursting time refers here to the time required to fill the driver before diaphragm bursting and does not refer to the time which the diaphragm takes to open fully. The data for these experiments were obtained at a p_5 of around 5, 20, and 30 bar and T_5 between 1350 and 1580 K. Ar and He were used as driven and driver gases, respectively.

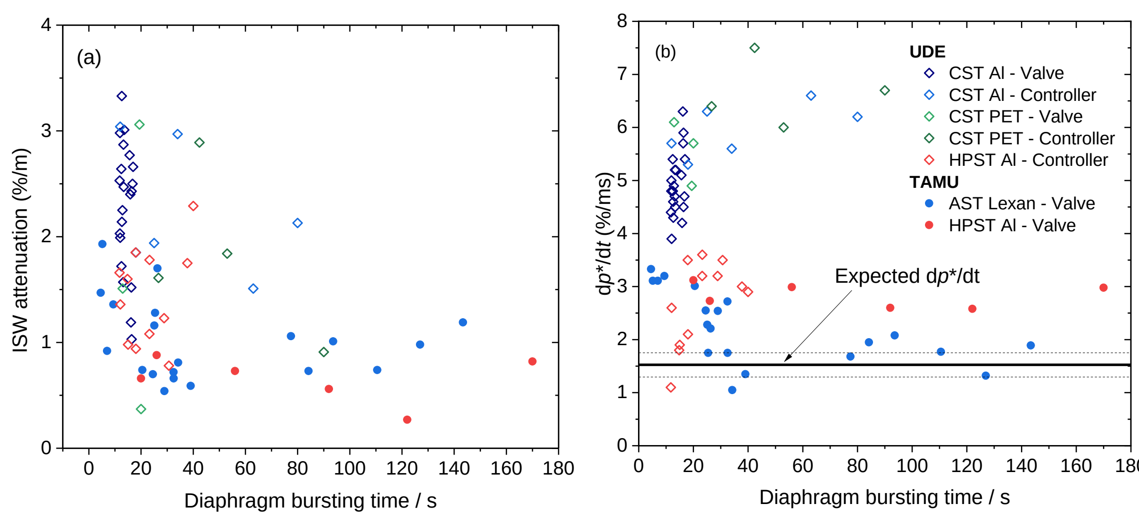

Figure 2. (a) ISW attenuation dependence on diaphragm bursting time, (b) dp*/dt dependence on diaphragm bursting time. Diamonds and circles are for UDE and TAMU data, respectively. Color codes correspond to filling methods and pressures.

Figure 2 shows attenuation data from UDE with relatively short bursting times (< 20 s), corresponding to the general procedure used in that laboratory. At TAMU, the general procedure involves longer filling times (> 60 s). The data collected with aluminum diaphragms show no bursting-time dependence for both laboratories at pressures around 5 bar (CST and AST data). However, the polycarbonate diaphragm

(Lexan) data from TAMU approach a clear limit at longer bursting times, with greater-than-expected values of dp*/dt and attenuation at very short bursting times. UDE conducted experiments with a similar material, PET, to replicate this effect, but no significant change in dp*/dt was observed. It should be noted that TAMU uses polycarbonate diaphragms paired with a cutter, whereas UDE generally uses aluminum.

TAMU utilizes aluminum diaphragms mainly for high-pressure experiments, therefore, a set of higher-pressure experiments were run at a similar Mach number. A series of measurements at high pressure were also run at UDE. No significant effect of the bursting time on either the attenuation or the dp*/dt was observed at TAMU, but the dp*/dt is much lower for fast filling for the UDE-HPST. The dp*/dt seems even to increase with the filling time of the driver section presuming a more ideal opening of the diaphragm at fast filling. It should be noted that the aluminum diaphragm for high-pressure runs from UDE are scored with a two-line cross pattern (thickness of the membrane = 2.5 mm and 0.61 mm ≤ cross depth ≤ 1.25 mm). As dp*/dt and ISW attenuation are apparent for smaller-diameter shock tubes, the effect seen at TAMU may not be apparent at UDE as the boundary-layer phenomena dominate. This effect may not be seen when using aluminum diaphragms at TAMU due to the increased pressure. The result of the different filling methods are also shown in Fig. 2, where metering the gases via a needle valve and a flow controller are compared. More scatter is seen at short bursting times for the needle valve. For longer bursting times, similar scatter is seen between the needle valve and flow controller. Overall, more repeatability of non-idealities is seen in the larger TAMU shock tubes for standard filling procedures (longer bursting times).

3 Discussion

A correlation for the attenuation data collected in this study was made as a function of initial pressure (p_1), initial temperature (T_1), ISW Mach number (M_1), ratio of specific heats of the test gas (γ_1), and ID of the shock tube (d); this correlation is depicted in Fig. 3.

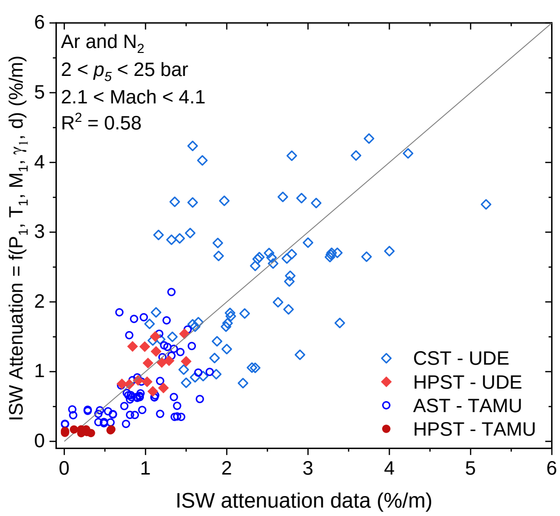

Figure 3. Correlation of attenuation data as a function of ID, incident shock Mach number, initial pressure, initial temperature, and test-gas specific heat ratio. The correlation is given as: ISW atten. $= e^{-23.03} p_1^{-0.89}\, T_1^{-3.52} \mathrm{M}_1^{-3.88} \gamma_1^{2.53} \mathrm{d}^{-1.86}$

Initial pressure, ISW Mach number, and the ratio of specific heats were all chosen based on their influence on the boundary-layer growth and driven-tube diameter was chosen to include the facility dependence.

These variables have the greatest significance on the correlation as they are directly related to the relative size of the boundary layer behind the ISW. Initial temperature was also chosen since there was a slight difference seen between facilities namely the UDE-HPST, which operated with an initial temperature around 323 K whereas the other facilities operated around 295 K. The inclusion of T_1 helped to improve the correlation, however, the importance of this parameter on the boundary-layer growth needs additional research. Further investigations including other facilities are also needed to improve this correlation; however, due to the scatter in the original data, further improvement may be difficult.

4 Conclusions and Future Work

A study was performed to investigate the dependence of shock-tube non-ideality on the operation of shock-tube facilities, particularly for the incident shock wave (ISW). Experiments were conducted in four shock tubes, two from UDE and two from TAMU. Attenuation data were collected in Ar and N_2 across a range of pressures and ISW Mach numbers. The result of this study is a correlation which includes numerous variables, including shock-tube inner diameter, for the shock-tube facilities used in this study. An investigation into the dependence of non-ideal shock-tube behavior (dp^*/dt and ISW attenuation) on diaphragm bursting time was also conducted. A limiting case was seen for TAMU shock tubes when using polycarbonate diaphragms and a cutter, which follows previously established theory. Using metal diaphragms, manufactured to burst ideally, this effect was not observed. At very short bursting times, much scatter is observed for all facilities for both dp^*/dt and ISW attenuation. A bursting time dependence on the dp^*/dt was observed for the UDE-HPST presuming a more ideal opening of the aluminum diaphragm at lower bursting time. Further collaboration between UDE and TAMU is planned for investigation of non-ideal shock-tube behavior including more shock-tube facility aspects, such as diameter change.

5 Acknowledgments

This work was supported by the German Research Foundation within the DFG Project SCHU 1369/27 and the TEES Turbomachinery Laboratory.

References

[1] Mirels H (1963). Test Time in Low-Pressure Shock Tubes. Phys. Fluids 6: 1201.

[2] Mirels H (1964). Shock Tube Test Time Limitation Due to Turbulent-Wall Boundary Layer. AIAA J. 2: 84.

[3] Petersen EL (1998). A shock tube and diagnostics for chemistry measurements at elevated pressures with application to methane ignition (Ph.D Dissertation), Stanford Univ., Stanford, CA.

[4] Mark H. (1958). The Interaction of a Reflected Shock Wave with the Boundary Layer in a Shock Tube. NACA TM 1418.

[5] Petersen EL, Hanson RK (2001). Nonideal effects behind reflected shock waves in a high-pressure shock tube. Shock Waves 10: 405.

[6] Hargis JW, Petersen EL. (2017). Shock-Tube Boundary-Layer Effects on Reflected-Shock Conditions with and without CO_2. AIAA J. 55: 902.

[7] Amadio AR, Crofton MW, Petersen EL (2006). Test-time extension behind reflected shock waves using CO_2-He and C_3H_8-He driver mixtures. Shock Waves 16: 157.

[8] Hong Z, Pang GA, Vasu SS, Davidson DF, Hanson RK (2009). The use of driver inserts to reduce non-ideal pressure variations behind reflected shock waves. Shock Waves 19: 113.

[9] Campbell MF. (2014). Studies of Biodiesel Surrogates using Novel Shock Tube Techniques (Ph.D Dissertation), Stanford Univ., Stanford, CA.

[10] White DR. (1958). Influence of diaphragm opening time on shock-tube flows. J. Fluid Mech. 4: 585.

[11] Rothkopf EM, Low W (1974). Diaphragm opening process in shock tubes. Phys. Fluids 17: 1169.

[12] Hickman RS, Farrar LC, Kyser JB (1975). Behavior of burst diaphragms in shock tubes. Phys. Fluids 18: 1249.

[13] Vivanco JE (2014). A New Shock-Tube Facility for the Study of High-Temperature Chemical Kinetics (Master's Thesis), Texas A&M University, College Station, TX.

[14] Aul CJE (2009). An Experimental Study into the Ignition of Methane and Ethane Blends in a New Shock-Tube Facility (Master's Thesis), Texas A&M University, College Station, TX.

[15] Zabeti S, Fikri M, Schulz C (2017). Reaction-time-resolved measurements of laser-induced fluorescence in a shock tube with a single laser pulse. Rev. Sci. Inst. 88: 115105.

[16] Nativel D, Shu B, Herzler J, Fikri M, Schulz C (2019). Shock tube study of methane pyrolysis in the context of polygeneration, Proc. Combust. Inst. 37: 197.